Phonons and conduction in molecular quantum dots: Density functional calculations of Franck-Condon emission rates for bifullerenes in external fields

Connie Te-ching Chang, James P. Sethna, Abhay N. Pasupathy, J. Park, D. C. Ralph, and P. L. McEuen

Laboratory of Atomic and Solid State Physics (LASSP), Clark Hall, Cornell University, Ithaca, New York 14853-2501, USA

(Received 26 May 2006; revised manuscript received 1 December 2006; published 31 July 2007)

We report the calculation of various phonon overlaps and their corresponding phonon emission probabilities for the problem of an electron tunneling onto and off of the fullerene-dimer molecular quantum dots C_{72} and C_{140}, both with and without the influence of an external field. We show that the stretch mode of the two balls of the dumbbell couples most strongly to the electronic transition and, in turn, that a field in the direction of the bond between the two fullerene balls is most effective at further increasing the phonon emission into the stretch mode. As the field is increased, phonon emission increases in probability with an accompanying decrease in probability of the dot remaining in the ground vibrational state. We also present a simple model to estimate the effect of molecular size on the phonon emission of composite dimer molecules and compare the results with the complete analysis of C_{72} and the experimentally tested C_{140}. In our approach we do not assume that the Hessians of the molecule are identical for different charge states. Our treatment is hence a generalization of the traditional phonon overlap calculations for coupled electron-photon transitions in solids.

I. INTRODUCTION

Physics is full of examples of phonon-coupled quantum tunneling events. A classic example from the 1960s is the work done with trapped-electron color centers in the lattices of the alkali halides.[1] More modern examples include the study of how the mobility of interstitials in metals is modulated by coupling of the defect to the resulting distortion of the surrounding lattice[2] and the study of how the interchain hopping by polarons is affected by phonon interactions.[3] In these studies and others, the frequencies before and after the transition were assumed to be unchanged and only the coordinate about which the harmonic potential is centered shifts. Here, our use of the word *phonon*, traditionally used for plane-wave-like solutions in periodic crystals, for *vibrational normal mode* is in the same spirit in this context for which we use the term *quantum dot*, a macroscale object, for *molecule*.

Over the past several years, several experiments and theoretical studies[4–6] have been done where single molecules have been used as the medium for vibration-assisted tunneling. Some recent experimental examples are measurements done with scanning tunneling microscopes,[7,8] studies of single hydrogen molecules in mechanical break junctions,[9] and the investigations that have directly motivated this work, the three-terminal single-molecule transistor experiments[10,11] where a single molecule is deposited between two leads and is subjected to both a source drain and gate bias. This is done in the Coulomb blockage regime, where the bias is tuned so that sequential transport can occur and a differential conductance graph can be plotted. In many of these differential conductance graphs, in addition to the main lines due to the change in the charge state of the molecule, there are a series of sidebands thought to be caused by the coupling of the electron to the vibrational modes of the molecule.

Spectroscopy has long been utilized as a tool in both chemistry and physics to study the properties and structure of atoms and molecules. Different types of spectroscopy are used for different aims; optical spectroscopy, for example, studies the interaction of electromagnetic radiation with the sample while this paper addresses the differential tunneling spectroscopy described above. Franck-Condon factors[12] serve as a very good tool for analyzing the absorption and emission band intensities corresponding to vibrational levels in atoms and molecules.[15] Over the years, many such molecular vibrational spectra have been calculated and cataloged using Franck-Condon factors.[16,17] Single-molecule transistors offer an opportunity to apply the Franck-Condon principles to a new system. Because we are dealing with single molecules, we can calculate [using *ab initio* density functional theory (DFT)] the full vibrational profile of both the initial and final electronic states of the molecule and thus calculate the Franck-Condon intensities generally.

In this paper, we use a general theory for vibrational overlaps where the vibrational modes of both the initial and final electronic states of the molecule are considered. Charge-dependent Hessians and anharmonic potentials in the context of single-molecule transistors have been considered previously[18,19] where the molecule is assumed to have one dominant mode in each electronic state. In the field of chemical spectroscopy, this topic has been addressed[20] through a general consideration of the Franck Condon factors with Duschinsky rotation[21] and its refinements,[22,23] which allows for different frequencies and eigenvectors between different charged states. Our paper considers a realistic model of an *N*-atom molecule with $3N$ possible modes (for example, the bifullerene C_{72} with 216 possible modes; see Fig. 1) and allows the calculation of experimental scenarios by combining our formulation with results from density functional theory.

In Sec. II, we set up our Hamiltonian. In Sec. III, we outline our version of the phonon overlap calculations including the Duschinsky rotation. In Sec. IV, we outline our DFT numerical methods. Section VI calculates the zero-field overlaps. Section VII addresses the overlaps in a field. Section VIII introduces a simple two-ball-and-spring model for
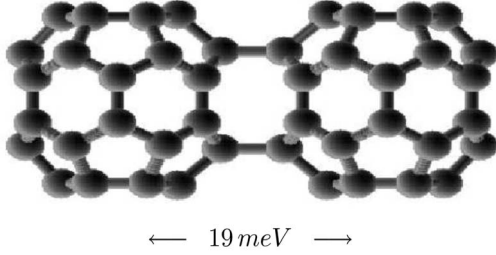
$\longleftarrow \quad 19 \, meV \quad \longrightarrow$

FIG. 1. C_{72} with 19-meV stretch mode indicated. In this high-symmetry viewpoint, some atoms are obscured behind others.

the behavior of the stretch mode overlap in the presence of a field. Section IX makes contact with dI/dV measurements of the entire spectrum, and Sec. X concludes.

II. HAMILTONIAN

Our Hamiltonian for the molecular dot is written in a mixed first and second quantized formulation

$$\mathcal{H} = \mathcal{H}^{lead} + \mathcal{H}^{dot} + \mathcal{H}^{tunnel}, \quad (1)$$

where $\mathcal{H}^{lead}$, $\mathcal{H}^{dot}$, and $\mathcal{H}^{tunnel}$ are given by the following:

$$\mathcal{H}^{lead} = \left[\sum_k \epsilon_k c_k^{l\dagger} c_k^l + \sum_k \epsilon_k c_k^{r\dagger} c_k^r \right], \quad (2)$$

$$\mathcal{H}^{dot} = \frac{1}{2} \mathbf{p}^\dagger \mathbf{M}^{-1} \mathbf{p} + (1 - c_d^\dagger c_d) \left[\frac{1}{2} (\mathbf{x} - \mathbf{r}_1)^\dagger \mathbf{K}_1 (\mathbf{x} - \mathbf{r}_1) \right]$$
$$+ c_d^\dagger c_d \left[\frac{1}{2} (\mathbf{x} - \mathbf{r}_2)^\dagger \mathbf{K}_2 (\mathbf{x} - \mathbf{r}_2) \right] + \epsilon_d c_d^\dagger c_d, \quad (3)$$

$$\mathcal{H}^{tunnel} = \sum_k T^l (c_k^{l\dagger} c_d + c_d^\dagger c_k^l) + \sum_k T^r (c_k^{r\dagger} c_d + c_d^\dagger c_k^r). \quad (4)$$

Here we do not incorporate explicit terms for spin and charging effects (as discussed, e.g., by Beenakker[24]); the phonon overlaps we calculate should also apply (with suitable modifications) in the presence of these electronic complications. Equation (2) describes the electronic component involving the left and right leads, Eq. (4) describes the tunneling component, and Eq. (3) describes the molecular vibrations (dot phonons) and the electronic state on the dot. Here $\mathbf{p}$ is the $3N$-component vector for the momentum of the N-atom molecule, $\mathbf{M}$ is the mass matrix (diagonal entries giving the masses of the different nuclei in groups of three), $\mathbf{x}$ is the $3N$-dimensional vector for the atomic coordinates of the molecule, $\mathbf{r}_1$ and $\mathbf{r}_2$ are the $3N$-dimensional vectors for the minimum energy configurations of the initial and final electronic states, and $\mathbf{K}_1$ and $\mathbf{K}_2$ are the quadratic forms giving the vibrational potential energy near $\mathbf{r}_1$ and $\mathbf{r}_2$. The 1 and 2 indices reference the charge state of the molecule. In our transition, the 1 index refers to the molecular state with the smaller number of electrons. $T^{l/r}$ is the tunneling matrix where the superscripts l and r specifies the left or right lead, where we for simplicity ignore dependence of T on the electron wavevector k. Finally, $c^\dagger$ and c are creation and destruc-

tion operators, respectively, for electrons. An external force $\mathbf{f}$ on the atomic coordinates shifts the ground state configuration: e.g., $\mathbf{r}_2 = \mathbf{r}_2^{(0)} + \mathbf{K}_2^{-1} \mathbf{f}$.

Although the phonon states can also be expressed in second-quantized form via the creation and annihilation operators for bosonic particles $a^\dagger$ and a, we chose to express them in first-quantized form to facilitate the calculation of the $3N$-dimensional overlap integrals between different vibrational states of our initial and final molecules.

III. PHONON OVERLAP INTEGRALS

Phonon overlap integrals arise in quantum transitions in a variety of contexts, as described in the Introduction. We are interested in transitions between two electronic states in a bifullerene molecule and how the transition is affected by the change in relaxation of the positions of the neighboring atoms. Within the Born-Oppenheimer approximation, the total wave function is described by $|\Psi(\mathbf{z}, \mathbf{x})\rangle = |\varphi_\mathbf{x}(\mathbf{z}) \phi(\mathbf{x})\rangle$, where $\mathbf{x}$ labels the nuclear coordinates as above and $\mathbf{z}$ labels the electron coordinates. Strictly speaking, the ground-state electron wave function depends parametrically on the nuclear positions $\mathbf{x}$, but for the bifullerenes the zero-point atomic fluctuations $\delta \mathbf{x}$ are on the order of picometers where tunneling matrix elements vary on angstrom scale. Hence we can assume $\varphi_\mathbf{x}(\mathbf{z}) \approx \varphi(\mathbf{z})$ and hence factor our wave function into a purely electronic component and a purely nuclear component. [This corresponds to the approximation in Eq. (4) that the tunneling matrix element $T^{l/r}$ is independent of the atomic positions $\mathbf{x}$.] A quantum transition mediated by a perturbing Hamiltonian $\mathcal{H}^{int}$ involving only electronic degrees of freedom [such as in Eq. (4)] will thus be given by

$$\mathcal{H}_{fi}^{int} = \langle \Psi_f(\mathbf{z}, \mathbf{x}) | \mathcal{H}^{int} | \Psi_i(\mathbf{z}, \mathbf{x}) \rangle = \langle \varphi^i(\mathbf{z}) \phi^i(\mathbf{x}) | \mathcal{H}^{int} | \varphi^f(\mathbf{z}) \phi^f(\mathbf{x}) \rangle$$
$$= \langle \varphi^f(\mathbf{z}) | \mathcal{H}^{int} | \varphi^i(\mathbf{z}) \rangle \langle \phi^f(\mathbf{x}) | \phi^i(\mathbf{x}) \rangle. \quad (5)$$

Conductance through our molecular quantum dot[23] demands an electronic transition onto the dot (potentially exciting vibrations), followed by a transition off of the dot. We imagine that these two transitions are incoherent, that the bottleneck is tunneling from the right lead onto the dot, and that the vibrational excitations thermalize before the next transition. For simplicity, we also assume zero temperature and low currents (so that nonequilibrium vibrational excitations may be ignored). All of these assumptions are thought to be fairly accurate for the experimental system.[25] With these assumptions, the conductance through the dot, expressed in Beenakker's notation,[24] is a sum of the conductances through parallel "channels" with different final phonon excitations

$$\text{conductance} \propto \sum_{E_p < eV} \Gamma_p^r \propto \sum_{E_p \leqslant eV} |\langle \phi_p^f(\mathbf{x}) | \phi^i(\mathbf{x}) \rangle|^2. \quad (6)$$

Here eV is the energy available to add an electron to the dot under external voltage V, $E_p = \epsilon_d + \Sigma_k p_n \hbar \omega_n$ is the energy of the eigenstate of the dot Hamiltonian [Eq. (3)] with p_n phonons emitted into mode n, and the conductance Γ_p^r from the right lead onto the dot through channel p involves the square of the matrix element $\mathcal{H}_{fi}^{int}$ of Eq. (5), and hence the square of the phonon overlap from the neutral ground state

ϕ^i into the excited vibrational state ϕ_p^f of the charged molecule. As each threshold step in bias is crossed, a new possible pathway becomes accessible and the square of its overlap must be added to the expression.

This expression for the conductance is used in calculations described in Sec. IX to predict *I-V* relations for the molecular quantum dot (see Fig. 10 below). The general theory[24,34–36] includes finite temperatures, more symmetric leads, and spin and charge effects. Nevertheless, the expressions for the rates Γ and phonon overlaps given above, with appropriate modifications for finite-temperature effects, are the same for the general and simplified models.

In recent experiments,[26] long phonon lifetimes extending at least 50 times beyond the lifetimes observed in Raman spectroscopy have been measured for experiments on suspended carbon nanotubes. However, the authors note that the lack of coupling to a substrate may account for this increase. In other experiments,[7] the experimental setup was arranged to increase the lifetime of the electron compared to the phonon, allowing for observation of transient vibronic levels. For our calculation, we presume that low currents and strong phonon coupling between molecule and leads ensures vibrational relaxation between electron tunneling events.

The phonon overlap integral is the quantity of interest since it modulates the total transition rate. Its value is a measure of the probability of occurrence of a particular transition between the initial vibrational state of the initial charge state (assumed to always be the ground state) and the final vibrational state of the final charge state. This quantity will suppress the total transition rate matrix element, leading to less intensity in the line. Summing over final states yields unity:[27]

$$\sum_f |\langle \phi^f(x)|\phi^i(x)\rangle|^2 = 1, \qquad (7)$$

with the individual terms representing the probability decomposition of the initial state in the eigenstates of the final potential. Hence the weight of the original electronic transition is spread among the phonon excitations.

A. Normal modes and phonon wave functions

In $3N$ dimensions, the phonon Hamiltonian for the initial charge state is

$$\mathcal{H} = \frac{1}{2}\mathbf{p}^\dagger \mathbf{M}^{-1}\mathbf{p} + \frac{1}{2}(\mathbf{x}-\mathbf{r}_1)^\dagger \mathbf{K}_1(\mathbf{x}-\mathbf{r}_1). \qquad (8)$$

For molecules with atoms of unequal mass, transforming from position space to normal modes becomes much simpler if we use the standard trick of rescaling the coordinates by the square root of the mass and shift the origin to $\mathbf{r}_1$, the equilibrium configuration of the initial charge state:

$$\mathbf{y} = \mathbf{M}^{1/2}(\mathbf{x}-\mathbf{r}_1). \qquad (9)$$

Hence,

$$\mathcal{H}_1 = \frac{\mathbf{\Pi}^\dagger \mathbf{\Pi}}{2} + \frac{1}{2}\mathbf{y}^\dagger \Omega_1 \mathbf{y}, \qquad (10)$$

where $\mathbf{\Pi}=\mathbf{M}^{-1}\mathbf{P}$ and $\Omega_i=\mathbf{M}^{-1/2}\mathbf{K}_i\mathbf{M}^{-1/2}$ is a matrix with dimensions of frequency *squared*.

Similarly, the phonon Hamiltonian for the final charge state is

$$\mathcal{H}_2 = \frac{\mathbf{p}^\dagger \mathbf{M}^{-1}\mathbf{p}}{2} + \frac{1}{2}(\mathbf{x}-\mathbf{r}_2)^\dagger \mathbf{K}_2(\mathbf{x}-\mathbf{r}_2)$$

$$= \frac{1}{2}\mathbf{\Pi}^\dagger \mathbf{\Pi} + \frac{1}{2}(\mathbf{y}-\mathbf{\Delta})^\dagger \Omega_2(\mathbf{y}-\mathbf{\Delta}), \qquad (11)$$

where

$$\mathbf{\Delta} = \mathbf{M}^{1/2}(\mathbf{r}_2-\mathbf{r}_1) \qquad (12)$$

is the rescaled atomic displacement due to the change in the charge state.

B. $3N$-dimensional wave functions and overlaps

In this section we calculate the transition rate from the neutral molecule's ground state to the ground state and the various singly excited vibrational states of the charged molecule. Our calculation of the Franck-Condon factors is thus the one-phonon emission special case of the more general Duschinsky rotation calculations in the chemistry literature.[22] We present it here partly because we find this special case physically illuminating and partly to introduce our notation. We present in the Appendix the more complex calculation of the Franck-Condon factor from the neutral ground state to a doubly excited vibrational charged state.

Using the Hermite polynomials associated with solutions to the harmonic oscillator $[H_1(x)=2x$ and $H_2(x)=-2+4x^2]$ and the expression for the excited wave functions, we have the $3N$-dimensional vibrational eigenfunctions

$$\Psi_0^{(1)}(\mathbf{y}) = N_1 e^{-(1/2\hbar)\mathbf{y}^\dagger \Omega_1 \mathbf{y}}$$

$$\Psi_0^{(2)}(\mathbf{y}) = N_2 e^{-(1/2\hbar)(\mathbf{y}-\mathbf{\Delta})^\dagger \Omega_2(\mathbf{y}-\mathbf{\Delta})}$$

$$\Psi_{1,\alpha}^{(2)}(\mathbf{y}) = N_2\sqrt{2\omega_\alpha/\hbar}[(\mathbf{y}-\mathbf{\Delta})\cdot\hat{\boldsymbol{\epsilon}}_\alpha^{(2)}]$$
$$\times\exp\left(-\frac{1}{2\hbar}(\mathbf{y}-\mathbf{\Delta})^\dagger \Omega_2(\mathbf{y}-\mathbf{\Delta})\right)$$

$$\Psi_{2,\alpha}^{(2)}(\mathbf{y}) = \frac{N_2}{2\sqrt{2}}H_2\{\sqrt{\omega_\alpha/\hbar}[(\mathbf{y}-\mathbf{\Delta})\cdot\hat{\boldsymbol{\epsilon}}_\alpha^{(2)}]\}$$
$$\times\exp\left(-\frac{1}{2\hbar}(\mathbf{y}-\mathbf{\Delta})^\dagger \Omega_2(\mathbf{y}-\mathbf{\Delta})\right). \qquad (13)$$

Here, the $\mathbf{\Delta}$ encapsulates the geometric reconfiguration of the molecule [Eq. (12)], the superscript denotes the initial (1) and final (2) charge states, the first subscript is the number of phonons emitted, and the second subscript (if any) is the phonon mode α into which they were emitted. The frequency of the phonon mode α is given by ω_α, and $\hat{\boldsymbol{\epsilon}}_\alpha^{(i)}$ is the orthonormal eigenvector of mode α for the molecule in the electronic state i.

The overlap between the two ground vibrational states is
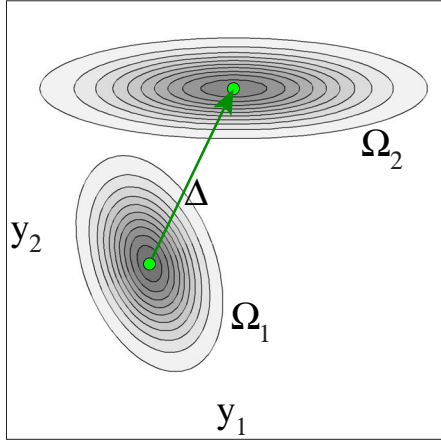
FIG. 2. (Color online) Wave functions $\Psi_0^{(1)}$ and $\Psi_0^{(2)}$ for harmonic potentials Ω_1^2 and Ω_2^2 in terms of a two-dimensional rescaled coordinate (y_1, y_2) separated by the rescaled length $\Delta = \sqrt{m}(\mathbf{r}_2 - \mathbf{r}_1)$. This and the succeeding figure (Fig. 3) are pictorial representations, with quadratic forms and displacements chosen to illustrate the variables used in the calculation.

$$O_{0,0} = \int d\mathbf{y} \Psi_0^{1*}(\mathbf{y}) \Psi_0^2(\mathbf{y})$$

$$= \int d\mathbf{y} \left\{ N_1 N_2 \exp\left(-\mathbf{y}^\dagger \frac{\Omega_1}{2\hbar} \mathbf{y}\right) \right.$$

$$\left. \times \exp\left(-(\mathbf{y}-\mathbf{\Delta})^\dagger \frac{\Omega_2}{2\hbar}(\mathbf{y}-\mathbf{\Delta})\right) \right\}. \quad (14)$$

We now rewrite expression (14) so that, rather than a product of two Gaussians (Fig. 2), it contains a single Gaussian (Fig. 3):

$$N_1 N_2 \int d\mathbf{y} [e^{-(1/2\hbar)\mathbf{y}^\dagger \Omega_1 \mathbf{y}} e^{-(1/2\hbar)(\mathbf{y}-\mathbf{\Delta})^\dagger \Omega_2 (\mathbf{y}-\mathbf{\Delta})}]$$

$$= \int d\mathbf{y} [e^{-(1/2\hbar)(\mathbf{y}^\dagger \Omega_1 \mathbf{y} + \mathbf{y}^\dagger \Omega_2 \mathbf{y} - \mathbf{y}^\dagger \Omega_2 \mathbf{\Delta} - \mathbf{\Delta}^\dagger \Omega_2 \mathbf{y} + \mathbf{\Delta}^\dagger \Omega_2 \mathbf{\Delta})}]. \quad (15)$$
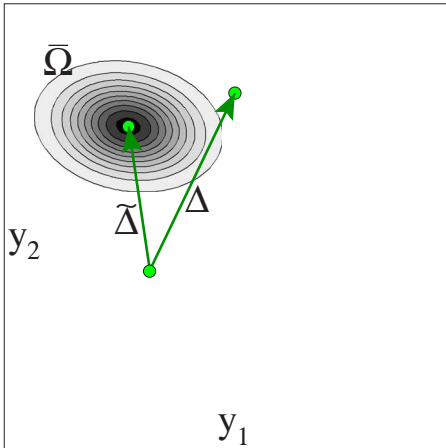
FIG. 3. (Color online) Overlap integrand corresponding to wave functions in Fig. 2, centered on $\widetilde{\Delta}$ with quadratic form $\bar{\Omega}^2$.

We want to express the single Gaussian as one that is centered on a new origin $\mathbf{y}_{max} = \widetilde{\Delta}$ with a new Hessian $\bar{\Omega}$ so that the integral is of the form

$$N_1 N_2 \int d(\mathbf{y} - \widetilde{\Delta}) e^{-(1/\hbar)(\mathbf{y}-\widetilde{\Delta})^\dagger \bar{\Omega}(\mathbf{y}-\widetilde{\Delta}) + B}, \quad (16)$$

which we know how to solve. Here B is one of the unknowns we are solving for, a constant which will be pulled out of the integral with a value given in Eq. (17).

Setting like quantities equal between expressions (15) and (16), we obtain

$$\widetilde{\Delta} = (\Omega_1 + \Omega_2)^{-1} \Omega_2 \Delta,$$

$$\bar{\Omega} = \frac{1}{2}(\Omega_1 + \Omega_2),$$

$$B = -\frac{1}{2}(\Delta^T \Omega_2 \Delta) + \frac{1}{2}\Delta^T \Omega_2 (\Omega_1 + \Omega_2)^{-1} \Omega_2 \Delta. \quad (17)$$

Our overlap integral now looks like

$$N_1 N_2 \int d\mathbf{y} [e^{-(1/\hbar)(\mathbf{y}-\widetilde{\Delta})^\dagger \bar{\Omega}(\mathbf{y}-\widetilde{\Delta})]}$$

$$\times e^{-(1/2\hbar)\Delta^\dagger \Omega_2 \Delta} e^{(1/2\hbar)\Delta^\dagger \Omega_2 (\Omega_1 + \Omega_2)^{-1} \Omega_2 \Delta}. \quad (18)$$

Rewriting the constant part of the integral in terms of $\widetilde{\Delta}$ and $\bar{\Omega}$, we have

$$N_1 N_2 \int d\mathbf{y} [e^{-(1/\hbar)(\mathbf{y}-\widetilde{\Delta})^\dagger \bar{\Omega}(\mathbf{y}-\widetilde{\Delta})}] e^{-(1/2\hbar)\Delta^\dagger \Omega_2 \Delta} e^{(1/\hbar)\widetilde{\Delta}^\dagger \bar{\Omega}\widetilde{\Delta}}. \quad (19)$$

Changing variables to $\widetilde{\mathbf{y}} = \mathbf{y} - \widetilde{\Delta}$, this last integral is another multidimensional Gaussian, equaling $1/\bar{N}^2$, where $\bar{N} = \sqrt[4]{\det\left(\frac{\bar{\Omega}}{\pi\hbar}\right)}$. The ground-state to ground-state overlap is then

$$O_{0,0} = \frac{N_1 N_2}{\bar{N}^2} \exp\left(\frac{1}{\hbar}\widetilde{\Delta}^\dagger \bar{\Omega}\widetilde{\Delta}\right) \exp\left(-\Delta^\dagger \frac{\Omega_2}{2\hbar}\Delta\right). \quad (20)$$

The probability of being left in the phonon ground state, the tunneling rate Γ, and the conductance are all suppressed by a factor $\exp(-G) = |O_{0,0}|^2$, where

$$G = -\ln(|O_{0,0}|^2). \quad (21)$$

This defines the total g factor which we will use to characterize the overall strength of the phonon coupling.

We can similarly calculate the overlap between the ground initial state and a final state with one phonon excited into mode α:

$$O_{0,1\alpha} = \int d\mathbf{y} \Psi_0^{(1)*}(\mathbf{y}) \Psi_{1,\alpha}^{(2)}(\mathbf{y} - \boldsymbol{\Delta})$$

$$= \int d\mathbf{y} \left\{ N_1 e^{-(1/2\hbar)\mathbf{y}^\dagger \Omega_1 \mathbf{y}} N_2 \sqrt{2\omega_\alpha/\hbar}[(\mathbf{y} - \boldsymbol{\Delta}) \cdot \hat{\boldsymbol{\epsilon}}_\alpha^{(2)}] \right.$$

$$\left. \times \exp\left(-\frac{1}{2\hbar}(\mathbf{y} - \boldsymbol{\Delta})^\dagger \Omega_2 (\mathbf{y} - \boldsymbol{\Delta}) \right) \right\}.$$

Combining the exponentials, rewriting them in terms of $\bar{\Omega}$ and $\tilde{\boldsymbol{\Delta}}$, we find

$$O_{0,1\alpha} = N_1 N_2 \int d\mathbf{y} \{ \sqrt{2\omega_\alpha/\hbar}((\mathbf{y} - \boldsymbol{\Delta}) \cdot \hat{\boldsymbol{\epsilon}}_\alpha^{(2)})$$

$$\times e^{-(1/\hbar)(\mathbf{y} - \tilde{\boldsymbol{\Delta}})^\dagger \bar{\Omega}(\mathbf{y} - \tilde{\boldsymbol{\Delta}})} e^{-(1/2\hbar)\boldsymbol{\Delta}^\dagger \Omega_2 \boldsymbol{\Delta}} e^{(1/\hbar)\tilde{\boldsymbol{\Delta}}^\dagger \bar{\Omega} \tilde{\boldsymbol{\Delta}}} \}. \tag{22}$$

Changing the variables to $\tilde{\mathbf{y}} = \mathbf{y} - \tilde{\boldsymbol{\Delta}}$, we have

$$O_{0,1\alpha} = N_1 N_2 \int d\tilde{\mathbf{y}} (\sqrt{2\omega_\alpha/\hbar} \{ [\tilde{\mathbf{y}} - (\boldsymbol{\Delta} - \tilde{\boldsymbol{\Delta}})] \cdot \hat{\boldsymbol{\epsilon}}_\alpha^{(2)} \}$$

$$\times e^{-(1/\hbar)(\tilde{\mathbf{y}})^\dagger \bar{\Omega}(\tilde{\mathbf{y}})}) e^{-(1/2\hbar)\boldsymbol{\Delta}^\dagger \Omega_2 \boldsymbol{\Delta}} e^{(1/\hbar)\tilde{\boldsymbol{\Delta}}^\dagger \bar{\Omega} \tilde{\boldsymbol{\Delta}}}$$

$$= N_1 N_2 \int d\tilde{\mathbf{y}} \{ \sqrt{2\omega_\alpha/\hbar}(\tilde{\mathbf{y}} \cdot \hat{\boldsymbol{\epsilon}}_\alpha^{(2)}) e^{-(1/\hbar)\tilde{\mathbf{y}}^\dagger \bar{\Omega} \tilde{\mathbf{y}}}$$

$$- \sqrt{2\omega_\alpha/\hbar}[(\boldsymbol{\Delta} - \tilde{\boldsymbol{\Delta}}) \cdot \hat{\boldsymbol{\epsilon}}_\alpha^{(2)}](1/\bar{N})^2 \}$$

$$\times e^{-(1/2\hbar)\boldsymbol{\Delta}^\dagger \Omega_2 \boldsymbol{\Delta}} e^{(1/\hbar)\tilde{\boldsymbol{\Delta}}^\dagger \bar{\Omega} \tilde{\boldsymbol{\Delta}}}.$$

Since the first term in the last integral is odd in $\tilde{\mathbf{y}}$, it must vanish.

Hence, from Eq. (20), the overlap between the ground initial state and the excited final state is

$$O_{0,1\alpha} = O_{0,0} \{ \sqrt{2\omega_\alpha/\hbar}[\hat{\boldsymbol{\epsilon}}_\alpha^{(2)} \cdot (\tilde{\boldsymbol{\Delta}} - \boldsymbol{\Delta})] \}. \tag{23}$$

We define

$$g_\alpha = \frac{|O_{0,1\alpha}|^2}{|O_{0,0}|^2} = \frac{P_\alpha}{P_{ground}} = \frac{\Delta I_\alpha}{\Delta I_{ground}}, \tag{24}$$

which experimentally gives the ratio of the current flowing emitting one phonon in mode α per electron to the current emitting zero phonons (the ratio of the step heights in the dI/dV curves). Thus,

$$g_\alpha = \{ \sqrt{2\omega_\alpha/\hbar}[\hat{\boldsymbol{\epsilon}}_\alpha^{(2)} \cdot (\tilde{\boldsymbol{\Delta}} - \boldsymbol{\Delta})] \}^2. \tag{25}$$

In the special case $\Omega_1 = \Omega_2$, where the change in charge state does not alter the spring constant matrices K_1 and K_2, the phonon frequencies and normal modes remain unchanged. It is well known that the total overlap integral is related to the one-phonon emission rates in a simple way: specifically $G = \Sigma_\alpha g_\alpha$. This is no longer the case when the two charge states have different spring constant matrices: we must calculate them explicitly.[21] The probability of multiple phonons being emitted into *distinct* phonon modes is given by $g_\alpha g_\beta \cdots |O_{0,0}|^2$, as it is for the traditionally studied case $\Omega_1 = \Omega_2$. But the probability for n phonons to be emitted into

the *same* final state is no longer $\frac{g_\alpha^n}{n!}|O_{0,0}|^2$. We do the calculation of two phonons in the Appendix; more general Duschinsky rotation calculations can be found in the literature.[22]

IV. METHODS

We used GAUSSIAN2003, a quantum chemistry package, to calculate all of the quantities needed in our calculation. These quantities include the force constant matrix K for different charge states of the molecule with dimension $3N \times 3N$. This matrix is related to the Ω matrix by the equation $K = M\Omega$ since in the cases of both C_{140} and C_{72}, M commutes with Ω. (Remember, in our notation, Ω is the frequency matrix *squared*.) We obtain the vibration frequency eigenvalues and normal-mode eigenvectors from Ω.

The program also gives the geometrically minimized structures of the molecule for its different charge states $\mathbf{r}$ and the forces on the atoms $\mathbf{f}$ under the influence of an external electric field.

All quantities are calculated under the hybrid B3LYP level of theory of the DFT model. Because we were working with molecules of considerable size and were calculating vibrational modes which require many electronic relaxation calculations, we used the minimal STO-3G basis set for our larger molecule ($N = 140$) and the slightly larger 3-21G* basis set for our smaller molecule ($N = 72$). Comparisons between the two basis sets for C_{72} suggest that the qualitative features are similar; more complete basis sets capture the polarization and charging effects more accurately which serve to increase our g factors since the variation between neutral and charged species are more pronounced. Our analytic approaches and their aim are independent of the details of the quantum chemistry calculation. All matrix calculations are done under MATLAB or its freeware clone GNU OCTAVE.

V. MOLECULES AND THEIR MODES

Our studies were inspired by work done by the McEuen and Ralph groups at Cornell and Berkeley.[10,11,25] Specifically, we looked at the single-molecule transistor made up of C_{140},[25] a molecule whose vibrational modes have been modeled and studied experimentally by Raman spectroscopy.[28] C_{140} is comprised of two C_{70} fullerene cages covalently bonded to each other via two C-C bonds. The dominant mode is the low-energy intercage vibration stretch mode at 11 meV shown schematically in Fig. 4. The second molecule studied was based on our interest in C_{140}. We wanted a molecule with similar properties to C_{140}, but with fewer atoms (C_{72}). The aim was to increase the accuracy of the basis set used for calculations which would be computationally costly with larger molecules.

Like C_{140}, the dominant excited mode was the intercage stretch mode which has an energy of 19 meV in C_{72}. The molecule is depicted in Fig. 1. Figures 1 and 4 were produced using GAUSSIAN2003 to minimize the geometry of the molecule and RASMOL to plot the atom positions.

For both molecules, the low-energy modes correspond to large-scale motion of the molecules such as the bending,
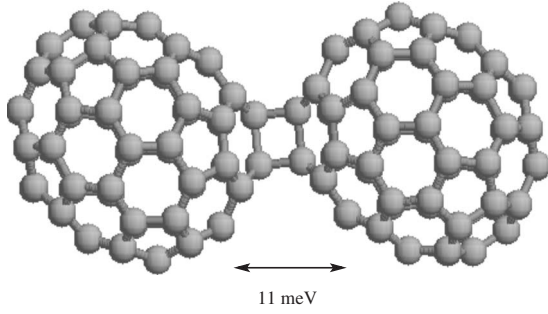
FIG. 4. C_{140} with stretch mode shown schematically.

11 meV

twisting, or stretching of the two cages with respect to each other (acoustic-type vibrations) while higher-energy modes correspond to motion of the atoms on a smaller scale (optical-type vibrations). For example, for C_{140} the 15-meV mode corresponds to a seesaw motion of the two cages with respect to each other and the 17-meV mode corresponds to a twisting motion of the two cages away from a central point, while the higher-energy 78-meV mode corresponds to simultaneous deformation of the cages themselves. The vibrations GAUSSIAN calculates are within 5% of the experimental values.

VI. BASIC QUANTITIES

The shift in the geometrically minimized structure of the C_{140} molecule as it acquires an extra electron is the predominant factor in determining the amount of phonon emission. If the structure changes little, the overlap between the two ground vibrational states of the initial and final charge states of the molecule will be larger, which suppresses phonon emission since the overlap is a mathematical statement of how likely it is for the molecule to remain in the ground vibrational state rather than transitioning to an excited vibrational state.

It is not known what the natural charge states of our molecule are on a gold substrate, as used in the experiments we compare to. A single C_{60} molecule typically has charge $-2e$ on gold; doubling this, we anticipate that the case of interest may involve a transition from perhaps four to five extra electrons on our molecule.

Table I is a chart of the change in the intercage distance

TABLE I. Change in distances ($\Delta \mathbf{r}$) between centers of mass of the fullerene cages for C_{140} during different charge transitions ($Q_1 \rightarrow Q_2$) where Q_1 is the initial charge state of the molecule and Q_2 is the final charge state of the molecule. Shown are the results of our DFT simulations and those of our simple model (Sec. VIII).

Transition $Q_1 \rightarrow Q_2$	DFT $\Delta \mathbf{r}$ [pm]	Simple $\Delta \mathbf{r} = x[Q_2] - x[Q_1]$
$0 \rightarrow 1$	1.005	3.16
$1 \rightarrow 2$	1.794	9.26
$2 \rightarrow 3$	2.333	14.8
$3 \rightarrow 4$	3.056	19.5
$4 \rightarrow 5$	3.7337	23.4

TABLE II. C_{72} undergoing different transitions. Probabilities and g factors for different transitions. For convenience we include columns 4 and 5; their result can be deduced from the second and third columns.

Transition	G	$g_{\alpha=stretch}$	$|O_{0,0}|^2$	$|O_{0,1\alpha=stretch}|^2$
$0 \rightarrow 1$	0.960	0.33	0.38	0.125
$1 \rightarrow 2$	1.18	0.406	0.31	0.126
$2 \rightarrow 3$	1.27	0.455	0.28	0.127
$3 \rightarrow 4$	1.29	0.492	0.27	0.135

between the two centers of masses of the fullerene cages upon adding an electron. As one can see, the distance increment increases as the charges increases. Therefore, as the charge on the molecule increases, the molecular incremental distortion $\Delta \mathbf{r}$ increases, and consequently the probability that the molecule will remain in the ground vibrational state after an electron has hopped on decreases, leading to stronger phonon sidebands in the differential conductance graphs. Table II gives, for each electronic transition of the molecule up to a charge state of four extra electrons, the total g factors [Eq. (21)] in the absence of an applied field, the g factor associated with the first excited state [Eq. (25)] where an intercage stretch-mode phonon is emitted, the probability of the molecule remaining in the ground state ($|O_{0,0}|^2$), and the probability that the molecule's final vibrational state is the first excited state of the stretch mode ($|O_{0,1\alpha=stretch}|^2$).

Plotting a graph of the g_α factor for the electronic transition of a neutral molecule to 1 molecule versus all 216 modes (as in Fig. 5) confirms that the stretch mode of the molecule dominates single-phonon emission. We also plot the corresponding graph of g_α for C_{140} in Fig. 6. As the charge state increases, the effects and phonon sideband strengths will increase.

Again, it is the stretch mode (whose identity is confirmed by displacing the equilibrium coordinates of the molecule by a distortion that is proportional to the eigenmode) that is important. Two-phonon emission may also be significant since experimentally[25] there is sometimes a second smaller peak at 22 meV which may be due to two-phonon emission
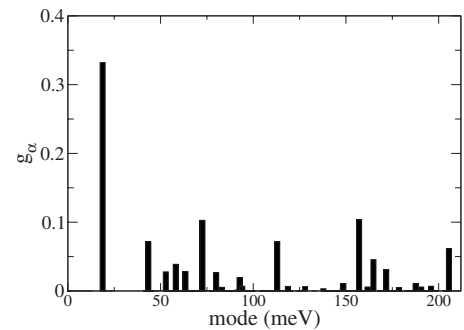
FIG. 5. g_α for the C_{72} $0 \rightarrow 1$ charge-state transition. The large peak is the stretch mode $\alpha = 10$ at 19 meV. Including the two-state emission lines would add an additional peak at 38 meV (twice the stretch mode) and an otherwise roughly continuous background (see Fig. 10).
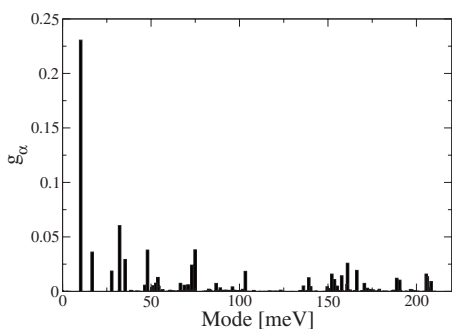
FIG. 6. g_α for the C_{140} $0 \to 1$ charge-state transition. The large peak is the $\alpha = 10$ stretch mode at 11 meV. Again, we estimate that the only significant two-phonon line is at 22 meV.

FIG. 7. $|\Psi|^2$ of the highest occupied molecular orbital level of C_{72} under an electric field of 4×10^9 V/m along an intercage bond, showing the polarization of the electron density.

into the same 11-meV mode. Two-phonon emission, however, yields a small contribution to the conductance. For two phonons emitted into the same mode, the contribution is given by the product of the single-phonon overlaps. For two phonons emitted into different modes, the contribution cannot be simply described by such a product and a complete expression obtained from integrating the product of the relevant multidimensional Gaussians is needed. Although we can calculate the probability of a transition to 2-phonon up to n-phonon vibrational final states, we confine ourselves to one-phonon emission in our calculations because, as will be illustrated in Fig. 10, two-phonon emission contributes a continuous background with the only sizable jump from the 11-meV mode.

VII. CONSIDERING EXTERNAL ELECTRIC FIELDS

In reality, the molecule is not in a vacuum but in a real environment of leads, substrate, and counter-ions. In the experiments,[11,25] there is a range of g factors for different experiments involving the same molecule. This implies that environmental effects play an important role and motivates our calculation of g factors in the presence of external fields. We account for one feature of this variable environment by applying an electric field to the system. This external field can come about as a result of image charges that are set up across the substrate or across the leads when extra electrons are added to the quantum molecular dot.

In the GAUSSIAN2003 program, we can impose an external field, relax the electronic wave function due to the induced polarization, and measure the force (expressed as a $3N$-vector, in this case a 216-vector) on each atom. The external field will polarize the charge on the molecule as seen in the following representation in Fig. 7 of the highest occupied molecular orbital under the influence of an external field along the intercage bond of the molecule (rendered using the freeware MOLDEN). This force will then act to distort the molecule's atomic configuration via lattice relaxation, leading to an increase in pathways available to the electron via vibration-assisted tunneling. The initial and final configurations in Eqs. (2)–(4) are $\mathbf{r}_1 = \mathbf{r}_1^{(0)} + \mathsf{K}_1^{-1} \mathbf{f}_1$ and $\mathbf{r}_2 = \mathbf{r}_2^{(0)} + \mathsf{K}_2^{-1} \mathbf{f}_2$, allowing us to calculate the g_α factors and hence the phonon emission rates from Eq. (25). Figure 8 shows that g_α for the
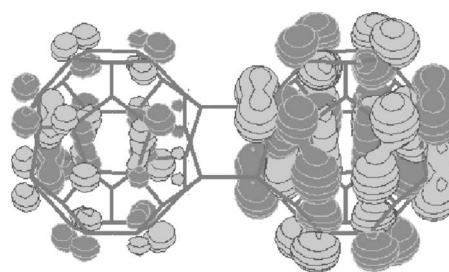
11-meV line for C_{140} increases substantially under an external field.

As can be seen in the plot, the field does increase the g factor from its bare value. At reasonable fields (those that we might expect to find in the experimental literature) such as the region where the field $\approx 3 \times 10^9$ V/m, g_α for the most represented mode (the stretch mode) increases to about 0.5. This field would correspond to a charge placed 7 Å away. And for a field corresponding to a charge placed 6 Å away (the closest plausible distance), g_α becomes around 1.0. However, in experiments, the g factor varies from values of much less than 1 to values as high as 6. In order to reach these quantities in our present theory, we would need to impose much higher and unphysical fields.

Another dependence we examined was the g-factor dependence of the various modes on the angle of a fixed electric field. In Fig. 9, the electric field was fixed at an extremely high value of 5×10^{12} V/m. The leftmost figure is the 11-meV mode—the stretch mode. Following it from left to right are the 3.7-meV mode magnified by a factor of 20 000, the 2.37-meV mode magnified by a factor of 20, the 15-meV mode magnified by a factor of 5, the 17-meV mode magnified by a factor of 200, and finally the 27.6-meV mode magnified by a factor of 500.

The molecule is oriented such that its long axis is aligned vertically. From the figure, we see that there is no coupling of the stretch mode (left shape) to the field when the field is aligned in a direction perpendicular to the stretch mode and that there is maximum coupling in the direction parallel to
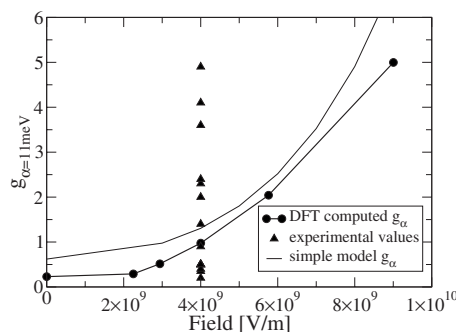
FIG. 8. Field dependence of g_α for the C_{140} 11-meV stretch mode from the DFT calculation. The solid line is the field dependence for our simple model calculation which is explained further in Sec. VIII. Experimental values (triangles) are taken at zero field, but included in the plot in a vertical column for visibility.
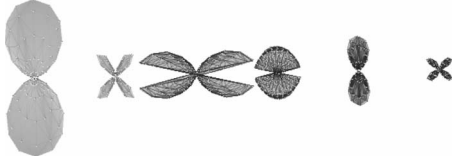
FIG. 9. Angle dependence of g_α for α giving the 11-meV stretch mode for C_{140}. Leftmost figure is g plotted as function of the angle of electric field (an extremely high field magnitude of 5×10^{12} V/m) for the 11-meV stretch mode; the remaining figures to the right are for other modes and have been magnified considerably to show their shape. The vertical represents fields along the long axis of the molecule. At more reasonable fields these distributions would be added to a roughly isotropic background.

the direction of the stretch mode. Note also that g_α is non-zero for α=stretch mode even in the absence of a field. The symmetries of the plots in Fig. 9 reflects the symmetry of the modes and how they relate to the symmetry of the applied field. C_{140} has C_{2h} symmetry, so it can be generated by a rotation of angle π around a fixed axis and a symmetry on a plane orthogonal to the fixed axis. The normal modes of a molecule also possess a definite symmetry with respect to the planes of symmetry of the molecule. The symmetry of the stretch mode is even under reflection in the $x-y$ plane, coinciding with the symmetry of the field E_x and orthogonal to the field E_z. Thus, the strongest coupling of the stretch mode is to E_x.

VIII. SIMPLE MODEL FOR OVERLAPS AND FIELDS

To what extent are these quantum overlaps a result of complex quantum chemistry (bonding and antibonding and electronic rearrangements inside the two cages)? Alternatively, how much can we understand from simple the electrostatics of dumbbells? By modeling the system simply as two rigid balls connected by a spring subject to an external field, we can obtain some understanding of how the dimensions of the problem as well as simple quantities might affect the overlap and g factor.

We write down the total energy of the system and then minimize the energy with respect to the parameters of our problem and in the presence of an external field—for our case we choose to minimize the charge on one ball and the distance x between the two balls.

The quantities we take into account are as follows:

$$E_{spring} = \frac{1}{2}K(x_2 - x_1 - a)^2,$$

$$E_{field} = q_1 E x_1 + q_2 E x_2,$$

$$E_{Coulomb} = \frac{k q_1 q_2}{(x_2 - x_1)},$$

$$E_{capacitance} = \frac{1}{2}\frac{k q_1^2}{r} + \frac{1}{2}\frac{k q_2^2}{r}, \tag{26}$$

where a is the equilibrium distance of the spring, x_1 and x_2 are the coordinates of the two balls, r is their radius, K is the

spring constant of the system, and k is the Coulomb constant.

We also note that $M_{total} = M_{ball_1} + M_{ball_2} = 2M_{ball}$ and $M_{red} = \frac{M_{ball_1} M_{ball_2}}{M_{ball_1} + M_{ball_2}} = M_{ball}/2$ are the well-known center of mass and reduced mass for the system. The last assignments we make are expressions for the charges on each ball (q_1 and q_2) in terms of the charges in the system:

$$q_1 = \frac{Q}{2} + \frac{q}{2},$$

$$q_2 = \frac{Q}{2} - \frac{q}{2}, \tag{27}$$

where Q is the total charge of the system and q is the difference between the charges on the two balls. The potential energy U then becomes

$$U = E_{spring} + E_{field} + E_{Coulomb} + E_{capacitance}$$

$$= \frac{1}{4r(a+x)}\{-2a^2 E q r + K[q^2(x-r) + Q^2(x+r)]$$

$$+ 2rx(2EQX - Eqx + kx^2)$$

$$+ a[K(q^2 + Q^2) + 2r(2EQX - 2Eqx + kx^2)]\}. \tag{28}$$

Here $x = x_2 - x_1$ is the relative distance between the two balls and $X = \frac{x_1 + x_2}{2}$ is the center of mass coordinates of the system. We next take the derivative of the potential with respect to q as the difference in charges on the two balls and set the resulting expression $\left(\frac{dU}{dq}\right)$ equal to zero. Solving this expression for q gives us the minimized distribution of charges on the balls under an external field:

$$q = \frac{Er(a+x)^2}{K(a-r+x)}. \tag{29}$$

Similarly, we take the derivative of the potential energy U with respect to the deviation of the stretch coordinate from equilibrium x, set this expression equal to zero, and solve for x. We keep terms up to second order in Q and E and get

$$x[Q] = AE^2 + BQ^2 + CE^2 Q^2, \tag{30}$$

where A, B, and C are given by

$$A = \left(\frac{2a^2 - 5ar - 3r^2}{4kK(a-r)^3}\right)ra^2,$$

$$B = \frac{K(a^2 + r^2 - 2ar)}{4a^2 k(a-r)^2},$$

$$C = \left(\frac{2r - a}{8k^2(a-r)^3}\right)r. \tag{31}$$

In Table I, we compare the $\Delta r = x[Q_2] - x[Q_1]$ in the absence of a field for our the simple model and the full DFT calculation discussed earlier where Q_1 is the total charge for the initial system and Q_2 is the total charge for the final system. The simple model has between 3 and 6 times the distortion of the quantum chemistry calculation, likely due to a combination of more effective screening of the Coulomb
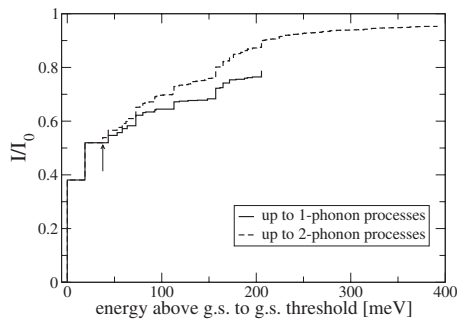
FIG. 10. *I-V* curve predicted for C_{72} for one-phonon processes (solid line) and up to two-phonon processes (approximate, dashed line), using the DFT STO-3G basis set. The arrow indicates the position of the two-phonon contribution from the stretch mode.

repulsion between cages and quantum chemistry effects in the latter.

The constants from Eq. (31) which define the expression for x in Eq. (30), in combination with the formula for the zero-point motion, $x_0 = \sqrt{\frac{\hbar}{M_{red}\omega_0}}$, and the one-dimensional equivalent of Eq. (25), give us an expression for G:

$$g = G = \frac{(x[Q_2] - x[Q_1])^2}{4x_0^2}, \tag{32}$$

where in this one-mode limit the $\ln G$ of the total overlap equals the one-phonon emission ratio g. Here M_{red} is equal to $\frac{70m_{carbon}}{2}$, $\omega_0 = \omega_{stretch} = 11$ meV and the zero-point motion x_0 for C_{140} is 2.17 pm.

Therefore, using these formulas our g factor for the $0 \rightarrow 1$ transition of C_{140} is 0.535 (and for C_{72} it is 0.92). The complete $3N$-dimensional calculations in the absence of a field for the same transition yield a g_α for the stretch mode of 0.23 for C_{140} (and 0.33 for C_{72}). This difference is not as large as one would expect from the difference in the center-of-mass motions: the 11-meV stretch mode incorporates motions that do not simply change the center-of-mass separation. In total, the many-body DFT calculations show a stretch-mode phonon emission about a factor of 3 smaller than that predicted from the simple physical model.

Finally, we compare the field dependence of the g_α between the simple model and the DFT calculation given in Fig. 8. The field dependence works out quite well. This simple model could be made more realistic by incorporating features from the DFT calculation (such as charging energies), but that would take us beyond our current illustrative goal.

IX. CURRENT DUE TO PHONON TRANSITIONS

Using the g factors corresponding to all of the different single-phonon modes, we plotted a current versus voltage graph for C_{72} using the simplified formula where all the phonons are identical in both charge states of the molecule. Figure 10 gives the current divided by I_0 versus the available energy above the ground-state to ground-state threshold for both one-phonon emission processes (solid line) and up to two-phonon processes (dashed line). The plots are con-

structed by iteratively calculating phonon emission from a pool of available energy. As energy decreases, less is available for emitting phonons. Our g_α's make use of the fact that the phonon quadratic forms Ω change between different charge states. As one can see, the currents due to one-phonon processes and for up to two phonon processes share similar gross features at the beginning such as the jump in current at the 19-meV energy mode corresponding to the stretch mode of the molecule. However, they start to deviate as the energy increases until they level off at different values of the current (0.8 for the one-phonon process and 0.95 for the two-phonon processes) which would seem to indicate that two-phonon processes will play a role in the *I-V* characteristics of a molecular quantum dot.

In addition, the *I-V* curve that includes all *n*-phonon processes will asymptote to 1. The two-phonon contribution forms almost a continuous background, except for $2\omega_{stretch}$, whose position is shown with an arrow in Fig. 10. We also note that the our treatment of two-identical-phonon emission is (for convenience) not the correct formula derived in Eq. (A14) which allows the frequencies to change between the initial and final states, but the approximate formulas given by Eqs. (33) and (34):

$$O_{0,2\alpha} \approx e^{-G} g_\alpha^2 / 2, \tag{33}$$

$$I/I_0(E) = \sum_\alpha \left[O_{0,1\alpha}\Theta(E - \hbar\omega_\alpha) + O_{0,2\alpha}\Theta(E - 2\hbar\omega_\alpha) \right]$$

$$+ \sum_{\alpha,\alpha' \neq \alpha} O_{0,1\alpha 1\alpha'}\Theta(E - \hbar\omega_\alpha - \hbar\omega_{\alpha'}). \tag{34}$$

X. CONCLUSION

There is much recent interest in vibrating mechanical systems coupled to electron transport on the nanoscale, from nanomechanical resonators[29,30] to single-electron shuttles.[31,32] Vibrational effects on electron transport through molecules have been studied since the 1960s in devices containing many molecules[33] and more recently have been shown to be important in transport through single molecules measured using scanning tunneling microscopes,[8] single-molecule transistors,[10,11] and mechanical break junctions.[9] In a natural extension of work done in the 1920s by Franck, Condon, and others in atomic spectra, we have studied the effects of molecular vibrations on electron transport through a molecule. We have shown that density functional theory calculations of the normal modes and deformations, coupled to a straightforward linear algebra calculation, can provide quantitative predictions for the entire differential tunneling spectrum, even including external fields from the molecular environment.

APPENDIX

Here we show how one can calculate the Franck-Condon factor for a transition from the neutral ground state to an excited state with one vibrational mode in a doubly excited state. (For emission into general excited states, we would need to use the appropriate multidimensional Gaussian multiplied by the appropriate Hermite polynomials. This calculation quickly becomes complicated,[22] and for the molecules of interest to us, multiple phonon emission is rare.) From the vibrational states given in Eq. (13), we are interested in the integral

$$O_{0,2} = \int d\mathbf{y} \Psi_0^{(1)*}(\mathbf{y}) \Psi_{2,\alpha}^{(2)}(\mathbf{y} - \mathbf{\Delta}), \qquad (A1)$$

where we can split the integral into two parts:

$$= \int d\mathbf{y} N_1 N_2 \sqrt{2} \omega_\alpha [\hat{\boldsymbol{\epsilon}}_\alpha^{(2)} \cdot (\mathbf{y} - \mathbf{\Delta})]^2 e^{-(1/2\hbar)(\mathbf{y}^\dagger \Omega_1 \mathbf{y})}$$
$$\times e^{-(1/2\hbar)[(\mathbf{y} - \mathbf{\Delta})^\dagger \Omega_2 (\mathbf{y} - \mathbf{\Delta})]} \qquad (A2)$$

$$- \int d\mathbf{y} N_1 N_2 \sqrt{2} \frac{1}{2} e^{-(1/2\hbar)(\mathbf{y}^\dagger \Omega_1 \mathbf{y})} e^{-(1/2\hbar)[(\mathbf{y} - \mathbf{\Delta})^\dagger \Omega_2 (\mathbf{y} - \mathbf{\Delta})]}. \qquad (A3)$$

Expression (A3) is just $-\frac{1}{\sqrt{2}} O_{0,0}$; we concentrate on expression (A2). First, as we did for the $O_{0,1}$ case, we rewrite this integral in terms of the quantities $\tilde{\mathbf{\Delta}}$ and $\bar{\Omega}$:

$$N_1 N_2 \sqrt{2} \left(\frac{\omega_\alpha}{\hbar}\right) \int d\mathbf{y} [\hat{\boldsymbol{\epsilon}}_\alpha^{(2)} \cdot (\mathbf{y} - \mathbf{\Delta})]^2 e^{-(1/\hbar)(\mathbf{y} - \tilde{\mathbf{\Delta}})^\dagger \bar{\Omega}(\mathbf{y} - \tilde{\mathbf{\Delta}})}$$
$$\times e^{-(1/2\hbar)\mathbf{\Delta}^\dagger \Omega_2 \mathbf{\Delta}} e^{(1/2\hbar)\tilde{\mathbf{\Delta}}(\Omega_1 + \Omega_2)\tilde{\mathbf{\Delta}}}. \qquad (A4)$$

We want to make this expression look like the known Gaussian integral: $C_1 \int dx x^2 e^{-x^2 + C_2}$ where C_1 and C_2 are constants. Changing the variables to $\tilde{\mathbf{y}}$,

$$\tilde{\mathbf{y}} = \mathbf{y} - \tilde{\mathbf{\Delta}},$$

$$d\tilde{\mathbf{y}} = d\mathbf{y},$$

$$\mathbf{y} = \tilde{\mathbf{y}} + \tilde{\mathbf{\Delta}}, \qquad (A5)$$

we rewrite the integral as one over $d^n \tilde{y}$:

$$N_1 N_2 \sqrt{2} \left(\frac{\omega_\alpha}{\hbar}\right) \int d\tilde{\mathbf{y}} [\hat{\boldsymbol{\epsilon}}_\alpha^{(2)} \cdot (\tilde{\mathbf{y}} + \tilde{\mathbf{\Delta}} - \mathbf{\Delta})]^2 e^{-(1/\hbar)\tilde{\mathbf{y}}^\dagger \bar{\Omega} \tilde{\mathbf{y}}}$$
$$\times e^{-(1/2\hbar)\mathbf{\Delta}^\dagger \Omega_2 \mathbf{\Delta}} e^{(1/2\hbar)\tilde{\mathbf{\Delta}}(\Omega_1 + \Omega_2)\tilde{\mathbf{\Delta}}}. \qquad (A6)$$

Expanding out the term in brackets in Eq. (A6), we get

$$[\hat{\boldsymbol{\epsilon}}_\alpha^{(2)} \cdot \tilde{\mathbf{y}} + \hat{\boldsymbol{\epsilon}}_\alpha^{(2)} \cdot (\tilde{\mathbf{\Delta}} - \mathbf{\Delta})]^2 = [\hat{\boldsymbol{\epsilon}}_\alpha^{(2)} \cdot \tilde{\mathbf{y}} + \mathbf{d}]^2 = (\hat{\boldsymbol{\epsilon}}_\alpha^{(2)} \cdot \tilde{\mathbf{y}})^2$$
$$+ 2\mathbf{d}(\hat{\boldsymbol{\epsilon}}_\alpha^{(2)} \cdot \tilde{\mathbf{y}}) + \mathbf{d}^2, \qquad (A7)$$

where $d = \hat{\boldsymbol{\epsilon}}_\alpha^{(2)} \cdot (\tilde{\mathbf{\Delta}} - \mathbf{\Delta})$.

The second term in Eq. (A7) will be zero in the integral because of symmetry considerations which dictate that odd-powered Gaussian integrals of the form $\int dx x^n e^{-x^2}$, where n is odd, always equal zero. The only terms in the integral of Eq. (A6) that remain are the first term and the constant $\mathbf{d}^2$.

We transform this integral into the appropriate normal-mode basis. Since we are integrating over the coordinates centered on $\tilde{\mathbf{\Delta}}$ for a system with a Hessian of $\bar{\Omega}$, we want to rewrite everything in terms of the eigenmodes of the averaged $\bar{\Omega}$. We will call these eigenmodes $\hat{\boldsymbol{\rho}}_\beta$ where the following definitions hold

$$\tilde{\mathbf{y}} = \sum_\beta p_\beta \hat{\boldsymbol{\rho}}_\beta,$$

$$\bar{\Omega} \hat{\boldsymbol{\rho}}_\beta = \bar{\omega}_\beta \hat{\boldsymbol{\rho}}_\beta. \qquad (A8)$$

Here, $\hat{\boldsymbol{\rho}}_\beta$ are the orthonormal eigenvectors for $\bar{\Omega}$ and p_β are the weightings of each mode's contribution to $\tilde{\mathbf{y}}$. Hence,

$$(\hat{\boldsymbol{\epsilon}}_\alpha^{(2)} \cdot \tilde{\mathbf{y}})^2 = \left(\sum_\beta p_\beta \hat{\boldsymbol{\epsilon}}_\alpha^{(2)} \cdot \hat{\boldsymbol{\rho}}_\beta\right)^2 = \sum_\beta p_\beta^2 (\hat{\boldsymbol{\epsilon}}_\alpha^{(2)} \cdot \hat{\boldsymbol{\rho}}_\beta)^2$$
$$+ \sum_{\beta \neq \beta'} p_\beta p_{\beta'} (\hat{\boldsymbol{\epsilon}}_\alpha^{(2)} \cdot \hat{\boldsymbol{\rho}}_\beta)(\hat{\boldsymbol{\epsilon}}_\alpha^{(2)} \cdot \hat{\boldsymbol{\rho}}_{\beta'}). \qquad (A9)$$

Again, the second term is odd in the new integration variables p_β and will be zero. Rewriting the integral in $d\vec{p}$ and remembering that $\hat{\rho}$ diagonalizes $\bar{\Omega}$, the integral from Eqs. (A1) and (A6) becomes

$$N_1 N_2 \sqrt{2} \left(\frac{\omega_\alpha}{\hbar}\right) \left[\int d^n p \sum_\beta p_\beta^2 (\hat{\boldsymbol{\epsilon}}_\alpha^{(2)} \cdot \hat{\boldsymbol{\rho}}_\beta)^2 \exp\left(-\frac{1}{\hbar} \sum_{\beta'} p_{\beta'}^2 \omega_{\beta'}\right) \right] e^{-(1/2\hbar)\mathbf{\Delta}^\dagger \Omega_2 \mathbf{\Delta}} e^{(1/2\hbar)\tilde{\mathbf{\Delta}}(\Omega_1 + \Omega_2)\tilde{\mathbf{\Delta}}}$$

$$= N_1 N_2 \sqrt{2} \left(\frac{\omega_\alpha}{\hbar}\right) \sum_\beta (\hat{\boldsymbol{\epsilon}}_\alpha^{(2)} \cdot \hat{\boldsymbol{\rho}}_\beta)^2 \left[\int d^n p p_\beta^2 \exp\left(-\frac{1}{\hbar} \sum_{\beta'} p_{\beta'}^2 \bar{\omega}_{\beta'}\right) \right] e^{-(1/2\hbar)\mathbf{\Delta}^\dagger \Omega_2 \mathbf{\Delta}} e^{(1/2\hbar)\tilde{\mathbf{\Delta}}(\Omega_1 + \Omega_2)\tilde{\mathbf{\Delta}}}. \qquad (A10)$$

But $\int x^2 e^{-Ax^2} dx = \frac{\sqrt{\pi}}{2A^{3/2}} = \frac{1}{2A} \int e^{-Ax^2} dx$, so

$$\int d^n p \, p_\beta^2 \exp\left(-\frac{1}{\hbar}\sum_{\beta'} p_{\beta'}^2 \bar{\omega}_{\beta'}\right) = \frac{1}{2\bar{\omega}_\beta/\hbar}\sqrt{\frac{\pi\hbar}{\bar{\omega}_\beta}}\prod_{\beta'\neq\beta}\sqrt{\frac{\pi\hbar}{\bar{\omega}_{\beta'}}}$$

$$= \frac{\hbar}{2\bar{\omega}_\beta}\frac{1}{\bar{N}^2}. \qquad (A11)$$

Hence, the first term in Eq. (A7) from Eq. (A10) becomes

$$N_1 N_2 \sqrt{2}\left(\frac{\omega_\alpha}{\hbar}\right)\sum_\beta (\hat{\boldsymbol{\epsilon}}_\alpha^{(2)}\cdot\hat{\boldsymbol{\rho}}_\beta)^2 \frac{\hbar}{2\bar{\omega}_\beta}\frac{1}{\bar{N}^2}e^{(1/\hbar)\tilde{\boldsymbol{\Delta}}^\dagger\bar{\Omega}\tilde{\boldsymbol{\Delta}}}e^{-(1/2\hbar)\boldsymbol{\Delta}^\dagger\Omega_2\boldsymbol{\Delta}}, \qquad (A12)$$

which from Eq. (20) we see is

$$O_{0,0}\sqrt{2}\omega_\alpha\sum_\beta \frac{1}{2\bar{\omega}_\beta}(\hat{\boldsymbol{\epsilon}}_\alpha^{(2)}\cdot\hat{\boldsymbol{\rho}}_\beta)^2. \qquad (A13)$$

Combining this with the third term from Eq. (A7) and expression (A3), our expression for the $0\rightarrow 2$ overlap becomes

$$O_{0,2_\alpha} = O_{0,0}\left\{\sqrt{2}\omega_\alpha\sum_\beta \frac{1}{2\bar{\omega}_\beta}(\hat{\boldsymbol{\epsilon}}_\alpha^{(2)}\cdot\hat{\boldsymbol{\rho}}_\beta)^2\right.$$

$$\left. + \sqrt{2}\left(\frac{\omega_\alpha}{\hbar}\right)[\hat{\boldsymbol{\epsilon}}_\alpha^{(2)}\cdot(\tilde{\boldsymbol{\Delta}}-\boldsymbol{\Delta})]^2 - \frac{1}{\sqrt{2}}\right\}$$

$$= O_{0,0}\left\{\sum_\beta \frac{\omega_\alpha}{\sqrt{2}\bar{\omega}_\beta}(\hat{\boldsymbol{\epsilon}}_\alpha^{(2)}\cdot\hat{\boldsymbol{\rho}}_\beta)^2\right.$$

$$\left. + \sqrt{2}\left(\frac{\omega_\alpha}{\hbar}\right)[\hat{\boldsymbol{\epsilon}}_\alpha^{(2)}\cdot(\tilde{\boldsymbol{\Delta}}-\boldsymbol{\Delta})]^2 - \frac{1}{\sqrt{2}}\right\}. \qquad (A14)$$

If $\Omega_1 = \Omega_2$ (i.e., there is no change in the harmonic potential), $\bar{\Omega} = \Omega_2$ and hence $\hat{\boldsymbol{\epsilon}}_\alpha^{(2)}\cdot\hat{\boldsymbol{\rho}}_\beta = \delta_{\alpha\beta}$ and $\bar{\omega}_\beta = \omega_\beta$. The first sum reduces to $\frac{1}{\sqrt{2}}$, canceling the last term. Therefore in this case

$$\left|\frac{O_{0,2\alpha}}{O_{0,0}}\right|^2 = 2\left(\frac{\omega_\alpha}{\hbar}\right)^2[\hat{\boldsymbol{\epsilon}}_\alpha^{(2)}\cdot(\tilde{\boldsymbol{\Delta}}-\boldsymbol{\Delta})]^4 = \frac{g_\alpha^2}{2}. \qquad (A15)$$

The change in harmonic potential upon charging the molecule allows for phonon emission even in the absence of a configurational shift. Therefore, even if $\boldsymbol{\Delta} = \tilde{\boldsymbol{\Delta}} = 0$, phonons can be emitted both because of frequency shifts ($\omega_\alpha \neq \bar{\omega}_\beta$) and because the normal modes change ($\hat{\boldsymbol{\epsilon}}_\alpha \neq \hat{\boldsymbol{\rho}}_\beta$).

The other overlaps could be performed in a similar way. The strategy is to write everything in terms of integrals of $\int dx \, x^n e^{-x^2}$ by transforming to the basis of the averaged Gaussian with $\bar{\Omega}$. The odd-powered integrals are eliminated and the even-powered terms remain.[34–36]

[1] J. H. Schulman and W. D. Compton, *Color Centers in Solids* (MacMillan, New York, 1962).

[2] C. P. Flynn and A. M. Stoneham, Phys. Rev. B **1**, 3966 (1987).

[3] E. M. Conwell, H. Y. Choi, and S. Jeyadev, J. Phys. Chem. **96**, 2827 (1992).

[4] D. Boese and H. Schoeller, Europhys. Lett. **54**, 668 (2001).

[5] S. Braig and K. Flensberg, Phys. Rev. B **68**, 205324 (2003).

[6] A. Mitra, I. Aleiner, and A. J. Millis, Phys. Rev. B **69**, 245302 (2004).

[7] X. H. Qiu, G. V. Nazin, and W. Ho, Phys. Rev. Lett. **92**, 206102 (2004).

[8] B. C. Stipe, M. A. Rezaei, and W. Ho, Science **280**, 1732 (1998).

[9] R. H. M. Smit, Y. Noat, C. Untiedt, N. D. Lang, M. C. van Hemert, and J. M. van Ruitenbeek, Nature (London) **419**, 906 (2002).

[10] H. Park, J. Park, A. K. L. Kim, E. H. Anderson, A. P. Alivisatos, and P. L. McEuen, Nature (London) **57**, 407 (2000).

[11] J. Park, A. N. Pasupathy, J. I. Goldsmith, C. Chang, Y. Yaish, J. R. Petta, M. Rinkoski, J. P. Sethna, H. D. Abruna, P. L. McEuen, and D. C. Ralph, Nature (London) **417**, 722 (2002).

[12] Franck was the first to suggest that an electronic transition can be accompanied by a vibrational excitation using classical arguments (Ref. 13). Condon later duplicated the argument using quantum mechanics and the Born-Oppenheimer approximation. (Ref. 14). According to Condon, the intensity of a particular transition can be determined by calculating the transition dipole moment. The electronic component can be factored out, leaving the square of the phonon overlap to modulate the total transition.

[13] J. Franck, Trans. Faraday Soc. **21**, 536 (1925).

[14] E. U. Condon, Phys. Rev. **32**, 858 (1928).

[15] G. C. Schatz and M. A. Ratner, *Quantum Mechanics in Chemistry* (Prentice Hall, Englewood Cliffs, NJ, 1993).

[16] G. Herzberg, *Molecular Spectra and Molecular Structure: I. Spectra of Diatomic Molecules* (Van Nostrand Reinhold, New York, 1950).

[17] J. B. Coon, R. E. Dewames, and C. M. Loyd, J. Mol. Spectrosc. **8**, 285 (1962).

[18] J. Koch and F. von Oppen, Phys. Rev. B **72**, 113308 (2005).

[19] M. R. Wegewijs and K. C. Nowack, New J. Phys. **7**, 239 (2005).

[20] A. Nitzan, Annu. Rev. Phys. Chem. **52**, 681 (2001).

[21] F. Duschinsky, Acta Physicochim. URSS **7**, 551 (1937).

[22] D. W. Kohn, E. S. J. Robles, C. F. Logan, and P. Chen, J. Phys. Chem. **97**, 4936 (1993).

[23] F. Chau, J. M. Dyke, E. P. Lee, and D. Wang, J. Electron Spectrosc. Relat. Phenom. **97**, 33 (1998).

[24] C. W. J. Beenakker, Phys. Rev. B **44**, 1646 (1991).

[25] A. N. Pasupathy, J. Park, C. Chang, A. V. Soldatov, S. Lebedkin, R. C. Bialczak, J. E. Grose, L. A. K. Donev, J. P. Sethna, D. C. Ralph, and P. L. McEuen, Nano Lett. **5**, 203 (2005).

[26] B. J. LeRoy, S. G. Lemay, J. Kong, and C. Dekker, Nature (Lon-

don) **432**, 371 (2004).

[27] L. I. Glazman and R. I. Shekhter, Sov. Phys. JETP **67**, 163 (1988).

[28] S. Lebedkin, W. E. Hull, A. Soldatov, B. Renker, and M. M. Kappes, J. Phys. Chem. B **104**, 4101 (2000).

[29] M. D. LaHaye, P. Buu, B. Camarota, and K. C. Schwab, Science **304**, 74 (2004).

[30] A. Naik, O. Buu1, M. D. LaHaye, A. D. Armour, A. A. Clerk, M. P. Blencowe, and K. C. Schwab, Nature (London) **443**, 193 (2006).

[31] L. Y. Gorelik, A. Isacsson, M. V. Voinova, B. Kasemo, R. I. Shekhter, and M. Jonson, Phys. Rev. Lett. **80**, 4526 (1998).

[32] A. Erbe, R. H. Blick, A. Tilke, A. Kriele, and J. P. Kotthaus, Appl. Phys. Lett. **73**, 3751 (1998).

[33] R. C. Jaklevic and J. Lambe, Phys. Rev. Lett. **17**, 1139 (1966).

[34] M. Buttiker, Y. Imry, R. Landauer and S. Pinhas, Phys. Rev. B **31**, 6207 (1985).

[35] C. W. J. Beenakkr and H. van Houten, *Solid State Physics: Semiconductor Heterostructures and Nanostructures* (Academic Press, Boston, 1991).

[36] R. Landauer, IBM J. Res. Dev. **1**, 233 (1957).